Chapter 6

The biodistribution and immuno-responses of differently shaped non-modified gold particles in zebrafish embryos

Chapter 6 highlights a study which demonstrates the capabilities of our TPMM in a real-case scenario. The study was performed in zebrafish embryos, where to two-photon excitation and the high temporal resolution enabled imaging of particle distribution in real-time.

This chapter is adopted from:
van Pomeren, M., Peijnenburg, W. J. G. M., Vlieg, R. C., van Noort, S. J. T. & Vijver, M. G. The biodistribution and immuno-responses of differently shaped non-modified gold particles in zebrafish embryos. Nanotoxicology 13, 558–571 (2019).

Author contributions:
M.V. conceived the research
M.v.P, M.P, R.V designed the experiments
M.v.P, M. P., R.V. carried out the experiments
M.v.P, M. P., R.V. analyzed the data.
R.V and S.J.T.v.N designed and build the microscope
M.v.P. wrote the manuscript with feedback from all authors
M.V. and J.v.N. supervised the research

6.1 PREFACE

For another application of the novel two-photon microscope technique we focus on the bio-distribution and immune-response of differently shaped gold nanoparticles (AuNPs) in zebra fish embryos. The unique properties of AuNPs make them interesting materials to work with, however their effects on the environment and on the health of organisms has yet to be fully understood. Imaging of AuNPs in live samples is difficult however by their weak one-photon luminescence brightness which impairs visibility in confocal microscopy. Confocal microscopy was used first to image fluorescently tagged macrophages, which are indicators of the immuno-response. However, to directly resolve where AuNPs are located in the zebrafish embryo, and whether they are being taken up by macrophages, a different imaging modality was required.

As gold nanoparticles feature impressive brightness upon two-photon excitation, as can also been seen in chapter 2 of this thesis, our two-photon multifocal microscope (TPMM) was especially well suited for measuring their distribution. Imaging the tail of the embryo we could discern individual spots, likely originating from single AuNPs, in real-time. Moreover, the high temporal resolution allowed us to image a macrophage which had taken up numerous NPs as it travelled along an artery wall. Direct imaging of AuNP macrophage uptake corroborated the confocal images, visualizing the first response of the immune system of the embryo reacts to the AuNPs and actively tries to dispose them.

These results illustrate how real-time imaging combined with two-photon excitation can provide insight in fast (biological) processes which would normally be eluded from detection. Moreover, it further shows how NPs are excellent contrast agents in two-photon microscopy. Overall, TPMM is an excellent imaging modality to obtain a more detailed understanding of the pathological effects of nanoparticles, like AuNPs, in live organisms.

6.2 INTRODUCTION

A central paradigm of toxicology is that toxic effects induced by a xenobiotic are due to a cascade of processes including Adsorption at sites of uptake, Distribution to target organs where the toxicant potentially induces a response, and ultimate storage in either the target organ or in any other organ, followed by Metabolization and Excretion (ADME)[1]. To make the chain of events even more complicated, it is to be acknowledged that different chemicals commonly follow different pathways, although they might end up in the same storage organ or tissue[2]. The myriad of processes may lead to various adverse effects, which makes it important to understand the mechanistic pathways and the main parameters affecting toxicity. While *in vitro* assays provide only limited information about the ADME of compounds, *in vivo* studies such as with zebrafish embryos provide more in depth insights[3] because cells in living organisms communicate and are specialized to perform specific essential functions. Using either *in vitro* or *in vivo* methods, it is key to understand the factors influencing (parts of) the ADME of xenobiotic compounds.

In the case of nanoparticles (NPs), uptake across epithelial membranes is dictated (among other factors) by size, shape and surface charge [4]. Just as for size [4], both the shape of particles as well as the accessory surface area influence how particles behave in exposure media [5]. Particle aggregation and dissolution for those particles that can dissolve (which is not the case for gold nanoparticles (AuNPs)) are in general the most important fate-determining processes. While size has been shown to influence uptake and biodistribution in zebrafish embryos [6,7] the impact of different nano-shapes on biodistribution is less investigated. Particle shape can be an important factor for cellular uptake, circulation time within the organism, and subsequently the biodistribution of nanoparticles [5]. In general, small, elongated nanoparticles are more easily taken up by cells than large and flat individual, non-aggregated particles [8]. This same tendency was found for the endpoint of biodistribution, as nanorods distributed throughout tumor tissues, whereas gold spheres and discs were located only at the surface of the tumor [9]. Moreover, the aspect ratio of rods was found to determine uptake and internal distribution: short rods were taken up faster and were trapped in the liver, while longer rods with a smaller aspect ratio showed lower uptake efficiency and were trapped in the spleen of mice [10–12]. Additionally, sharp gold nanostars can pierce the membranes of endosomes and escape to the cytoplasm regardless of their surface chemistry, size or composition [11,13].

As a noble metal with low toxicity, gold has been an ideal material in nanomedicine for diagnostic and therapeutic purposes such as imaging agents and drug-delivery systems [11,14,15]. Specifically coating/labeling the gold nanoparticles enables researchers to guide the particles to the desired target [9]. What happens to the gold nanoparticle when the coating or labeling is released is hardly studied, although some studies found that the coating can change [16] and even separate from the particles [17] under *in vivo* conditions. Gold is found to be biocompatible [15,18],

and its nanoform is categorized as an active and insoluble material which promotes cellular effects and/or mobility in organisms [19]. Therefore, it can be used as a platform for delivery in nanomedicine and for *in vivo* imaging experiments without major adverse effects. Due to their distinctive plasmonic resonances [20], high Rayleigh scattering [18], and resistance against photo-bleaching and photo-blinking [20], are gold particles very suitable for a variety of imaging techniques. Additionally, gold particles can be synthesized relatively easily, with control of their size and shape [20]. The fact that gold nanoparticles are synthesized in different shapes, combined with their inert properties makes gold the perfect material for testing the effect of shape on particle toxicity.

In this study, we aimed to determine the biodistribution and subsequent adverse responses to differently shaped, non-modified gold particles in zebrafish embryos. We used the word trafficking for active movement across the body of the organism, and the word biodistribution for where the AuNPs are located in the ZF embryo at a given time (static measurement 48 hours after exposure). The underlying research questions were:

1. Do differently shaped AuNPs induce different biodistribution patterns and hence do they accumulate in different target organs?

To answer this research question, the biodistribution of AuNPs was measured after 2 days of NP exposure. Our assumption is that once particles are accumulated in organs, due to agglomeration they are no longer available for biodistribution since biodistribution is limited to particles and agglomerates smaller than 250 nm [21]. By imaging after 2 day of exposure the AuNPs can be visualized in the target organs as sufficient uptake of AuNPs is expected to have taken place after this exposure duration without experiencing any morphological malformation [14,20].

2. What type of trafficking can we identify for AuNPs?

In general, nanoparticle clearance can occur via the hepatobiliary pathway or via the kidneys [22]. For the first pathway, uptake by macrophages is essential, whereas clearance via the urine occurs without intervention of macrophages. By tracking the movement of particles directly after internalization (simulated by microinjection), the initial clearance mechanism of the organism can be visualized.

3. Is the difference in biodistribution patterns also reflected in different response patterns?

As shown by previous research [23], immune responses, both local and systemic, are valuable endpoints for monitoring biodistribution. We therefore investigated the extent of recognition of the particles by neutrophils and macrophages.

4. Is the exposure to AuNPs also translated into effects on the behaviour of hatched zebrafish embryos?

In ecotoxicology, assessment of the behavioral response of hatched zebrafish embryos after exposure is a commonly used sub-lethal and sensitive apical endpoint [24]. By investigating sensitive sub-lethal endpoints, early signs of toxicity can be detected.

6.3 MATERIALS AND METHODS

Preparation of particle suspensions. Gold nanospheres and nano-urchins with nominal sizes of 60 nm were purchased from Sigma Aldrich (Zwijndrecht, The Netherlands). The particles were suspended in 0.1 mM phosphate buffered saline. Gold nanorods with a nominal size of 40 x 60 nm, stabilized with polyvinylpyrrolidone and suspended in water, were purchased from Nanopartz Inc. (Loveland, USA). Gold nano-bipyramids with a nominal size of 45 x 140 nm were purchased from Nanoseedz, ltd. (Hong Kong, China). The bipyramids were stabilized with polyethylene glycol in water and rinsed before use with demineralized water. Exposure suspensions were prepared by adding the purchased stock suspensions to egg water (60 µg/ml Instant Ocean Sea Salt, Sera GmbH, Heinsberg, Germany). All dilutions were freshly prepared and sonicated for 10 minutes in an ultrasonic water bath (USC200T, VWR, Amsterdam, The Netherlands), after which the embryos were immediately exposed.

Physicochemical characterization. The size and morphology of the suspended AuNPs were characterized using transmission electron microscopy (TEM; JEOL 1010, JEOL Ltd., Tokyo, Japan) after 1 hour of incubation in egg water. Dynamic light scattering assessments were performed on a Zetasizer Nano-ZS instrument (Malvern Instruments Ltd, Malvern, UK) to detect the size distribution and zeta-potential of Au NP suspensions in egg water at 0 h, 1 h and 24 h.

Zebrafish husbandry. Zebrafish were handled as described by animal welfare regulations and maintained according to standard protocols (http://ZFIN.org). Adult zebrafish were maintained at 25 ± 5 ˚C in a 14 h: 10 h light-dark cycle. Fertilized zebrafish eggs were obtained from Caspar zebrafish (*Danio rerio*), MPEG1.4:mCherry/MPX:GFP zebrafish and KDRL:GFP zebrafish, dependent on the analysis.

Waterborne exposure of zebrafish embryos to AuNPs. The OECD guideline 157 for the standard ZebraFish Embryo Test-protocol [25] was modified as described by Van Pomeren, et al[7]. We used the exposure window from 3 days post fertilization (dpf) till 5 dpf, since this exposure window was found to be associated with the highest amount of uptake[7]. Embryos were exposed to nominal concentrations of 5 mg/L. At this concentration, we expect to obtain sufficient signal for imaging while not observing any morphological malformations [14,20,27]. As a result, the concentration applied is expected to be too low to observe any sub-lethal effects as well.

Confocal microscopy. During the exposure period, Casper zebrafish embryos were examined daily to check fitness (malformations and mortality) using a dissecting microscope. During the final examination, embryos were rinsed three times with egg water, kept under anesthesia

(0.02% Tricaine, Sigma) in egg water and embedded with low melting agarose (CAS 39346-81-1, Sigma Aldrich, Zwijndrecht). Fitness was not affected during this inspection. Final examination was performed using the reflection of Au NPs according to the method described by Kim et al.[28] using a confocal microscope (Zeiss LSM5 Exciter).

Stereo fluorescence microscopy. Biodistribution and subsequent identification of target organs can be visualized by examination of the immune responses that are locally induced by the particles [23]. Similar to the analysis described above and applying the same exposure period, transgenic MPEG1.4:mCherry/MPX:GFP zebrafish embryos were examined daily. During the final examination, embryos were rinsed three times with egg water, kept under anesthesia (0.02% Tricaine, Sigma) in egg water and imaged in an agarose (CAS 9012-36-6**,** Sigma Aldrich, Zwijndrecht) covered Petri dish. Final examination was performed using the fluorescent signal of the fluorescent-labeled neutrophils (GFP) and the macrophages (mCherry) with a fluorescence stereo microscope (MZ 205 FA, Leica). Doing so, each image contains three channels: bright field, fluorescent green (GFPgreen/neutrophils), and fluorescent red (DRSred/macrophages). Using ImageJ software [29], images were assessed for fluorescence intensity and a corrected total cell fluorescence (CTCF) value was calculated [30].

Two photon multifocal laser microscopy. In order to investigate the clearance mechanism of the organism, the time dynamics of nanoparticles was tracked in order to follow the clearance. The time dynamics of particle trafficking was visualized with a two photon multifocal laser microscope [31]. For this, the particle with the most optimal optical properties was chosen, as this method is only suited for particles with a plasma resonance close to 830 nm. For our selection of particles, the nano-bipyramids showed to be best suited since their plasma resonance was 850 nm. A high, non-environmental relevant concentration (19 mg/L) was selected to guarantee good visibility. To assure particle presence in the organism, 3 day old transgenic KDRL:GFP zebrafish embryos were injected in the duct of Cuvier with 2nL nano-bipyramid gold NPs using a Femtojet injector (Eppendorf), half an hour prior to scanning. During the scanning, embryos were kept under anesthesia (0.02% Tricaine) in egg water while they were embedded in 0.4% low melting agarose. The success of the injections was assessed by looking at the absence of leakage to the yolk and the displacement of blood cells by injection-fluid.

Behavioral analysis. Since gold rarely induces lethal effects at the tested concentration, behavioral analysis was chosen as a more sensitive toxicity endpoint, as commonly used in neurotoxicity [24]. Before behavioral analysis, all living embryos (120 hpf) were evaluated in terms of normal development, morphological defects and vitality using a stereo dissecting microscope. The behavioral analysis was performed by subjecting the embryos to the light–dark challenge test as modified according to Hua et al.[23]. Low locomotor activity of zebrafish embryos occurred under light exposure (basal phase). A sharp spike of fast swimming activity

was induced by a sudden transition to dark, lasting less than 2 s (challenge phase)[23]. A total of 22 min of recording was used: 10 minutes acclimatization, 4 minutes basal phase, 4 minutes challenge phase and 4 minutes recovery phase. The total distance moved and the velocity of each zebrafish embryo was tracked using the Zebrabox (Viewpoint, Lyon, France) and analyzed using EthoVision software (Noldus Information Technology, Wageningen, The Netherlands).

Statistical analysis. Data of the behavioral test and the immune responses (represented as CTCF) were presented as mean ± standard error of the mean (SEM). The homogeneity of variance was checked using the SPSS 23 software package. The significance level for all calculations was set at $p<0.05$. Significant differences between the different exposures within each phase were tested using a one-way analyses of variance (ANOVA) with Tukey's multiple comparison post-test.

6.3 RESULTS

6.3.1 PHYSICOCHEMICAL CHARACTERIZATION

Using TEM images (Figure 6.1), size and shape of the particles were verified. According to the pictures, no large size deviations nor impurities were observed. This was in agreement with the information received from the producers.

Hydrodynamic size measurements obtained by means of DLS showed little variation over time (Table 6.1). This was with the exception of the nano-Au bipyramids as these particles did not follow this general pattern and formed aggregates immediately after preparation of the test suspension, which became even larger over time. This observation is probably related to the observation of the zeta potential being close to zero, which is indicative of lack of repulsive forces.

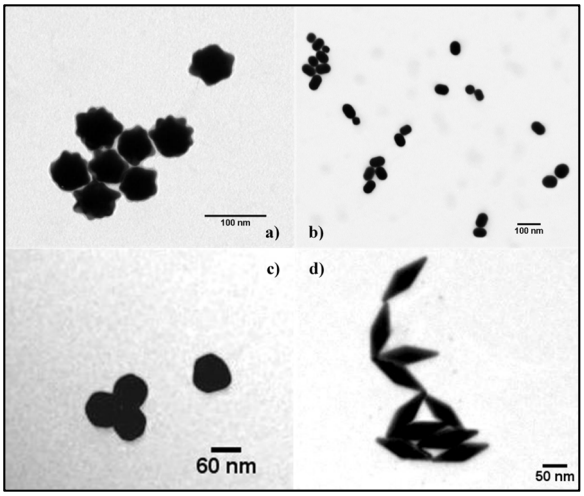

Figure 6.1: TEM images of the four tested nanogold particles. (a) nano-urchins (b) nanorods (c) nanospheres and (d) nano-bipyramids.

	Zeta potential (mV ± SD)				Size distribution (nm ± SD)		
	0h	1h	24h		0h	1h	24h
Nanosphere	-24 ± 2	-28 ± 4	-18 ± 5		74 ± 0	76 ± 2	79 ± 0
Nanorod	-27 ± 1	-28 ± 0	-11 ± 1		71 ± 0	73 ± 0	79 ± 3
Nano-urchin	-8 ± 1	-9 ± 0	-30 ± 1		88 ± 6	98 ± 6	72 ± 1
Nano-bipyramid	9 ± 1	3 ± 1	-4 ± 1		501 ± 45	1158 ± 151	5014 ± 2138

Table 6.1: Zeta potential and size distribution as measured by DLS of the different gold nanoparticles over time.

6.3.2 Biodistribution of AuNPs

Using a confocal laser-scanning microscope, clusters of nanoparticles could be visualized in exposed zebrafish embryos. Independent of the shape, every type of particle was observed to be present in the intestinal tract (examples of confocal images of particles in the intestinal tract can be found in the supplementary materials). Nanorods were found to efficiently distribute to other digestive organs of the embryo as well, such as the liver/gallbladder (Figure S6.1). For most of the particle shapes, clusters were also found in most probably a blood vessel near the eye (Figure 6.2).

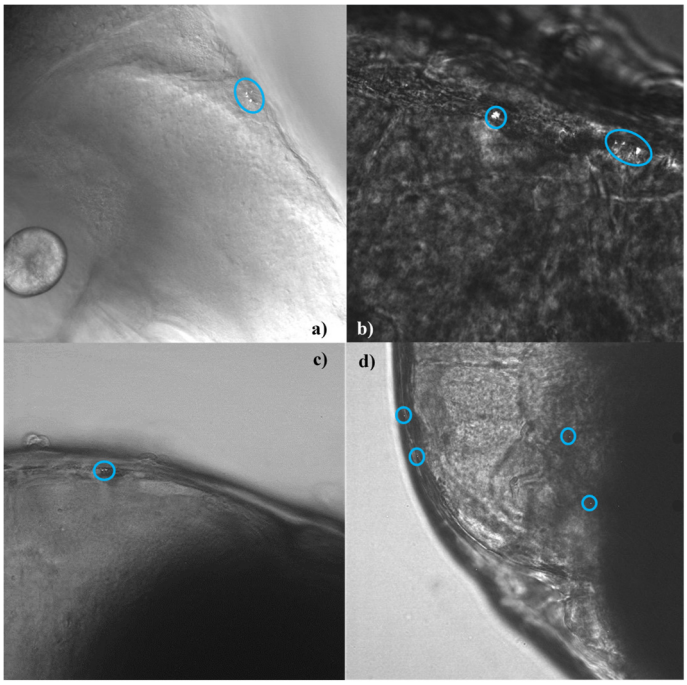

Figure 6.2: Confocal images showing particle clusters in blood vessels near the eye of the zebrafish embryo (5 dpf) for different nanogold particles. a) nanorods b) nano-urchins c) nanospheres and d) nano-bipyramids.

6.3.3 TRAFFICKING OF AUNPS

For the optical most optimal nanoparticles, the nano-bipyramids, the time dynamics of biodistribution were examined. After intravenous injection, the particles were found to be distributed throughout the tail of the embryo (Figure 6.3). As can be observed from Figure 6.3, free particles and clusters distributed through the bloodstream. Particles are thereafter phagocytosed by macrophages. A macrophage loaded with particles can be observed in the tissue (confirmed by the fluorescent signal), which moved over the tissue to the vein (Figure 6.3). From there, it will go to the liver or spleen to be cleared from the organism [33].

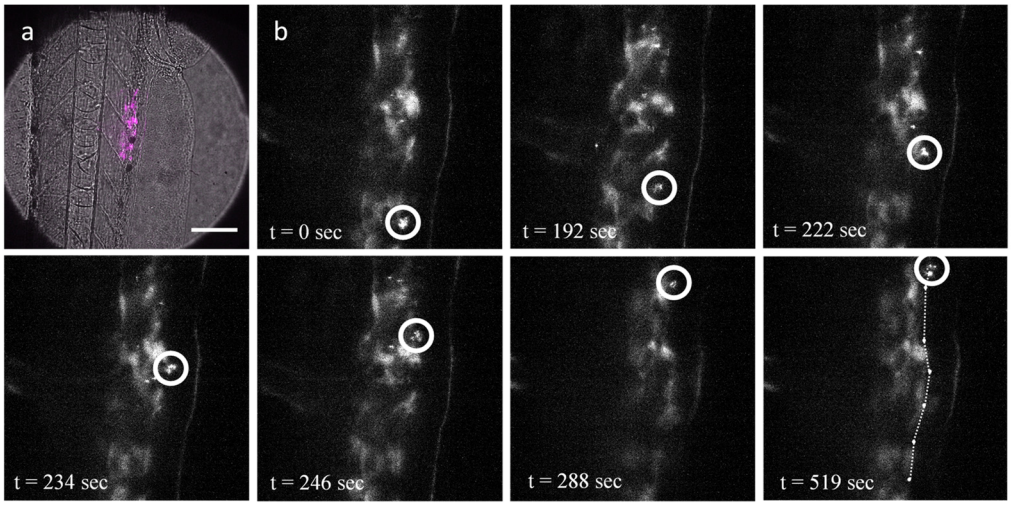

Figure 6.3: Macrophage filled with gold bipyramids moves along the artery wall after which it is released into the bloodstream. a) Transmission image with emission overlay (magenta) of the imaged region (scale bar 2 µm). b) Macrophage (white circle) moves along the artery wall, at t = 519 seconds the macrophage releases from the artery wall into the bloodstream.

6.3.4 IMMUNO-RESPONSES

Upon inspection of the response of the immune system of the whole organism and of responses in specific regions (Figure 6.4 and Figure S6.2), different response patterns were observed. In case of the neutrophils (Figure 6.4; a, c, e), the nano-urchins, nanorods and nano-bipyramids did not induce any visible effect on the immune system at the whole organismal scale (Figure 6.4a) and in the tail (Figure 6.4c).

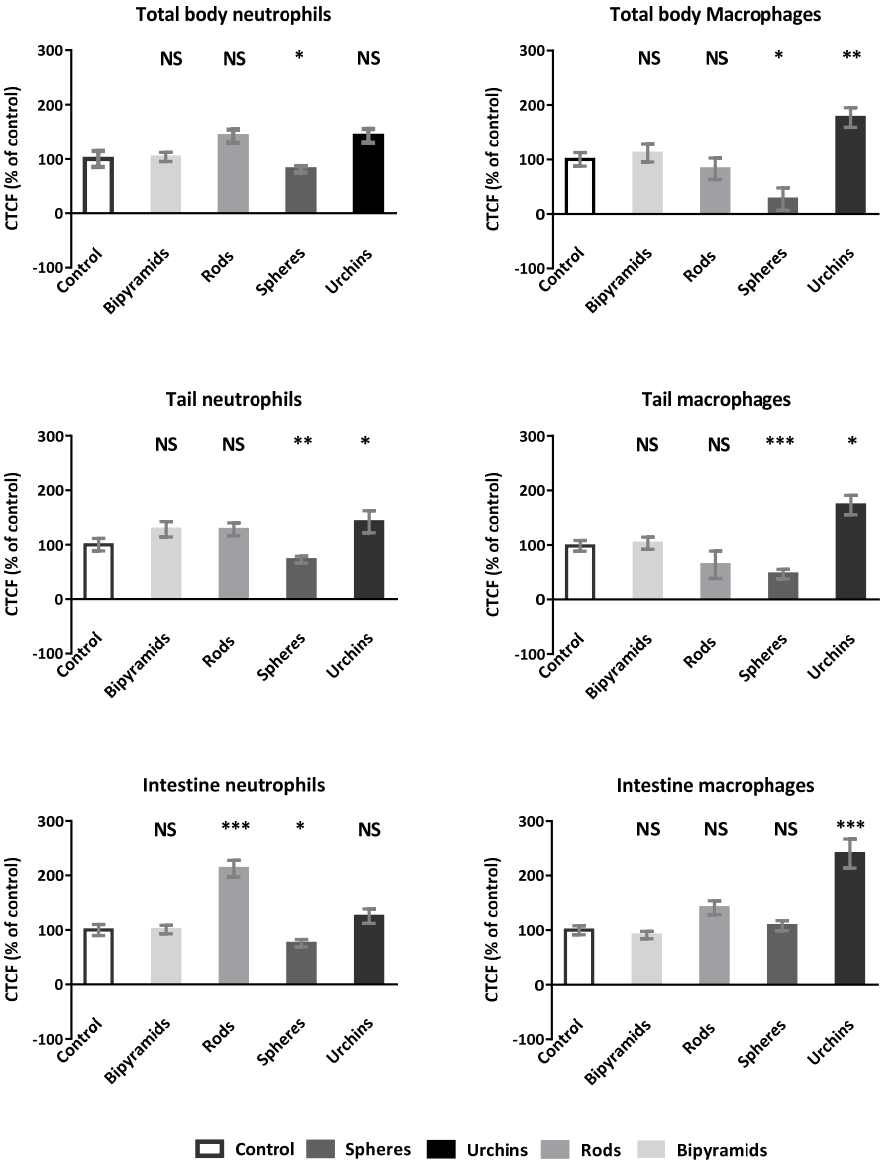

Figure 6.4: Abundance (relative to control) of neutrophils (a, c and e) and macrophages (b, d and f) in 5 dpf zebrafish embryos after exposure to differently shaped nanogold particles. The abundance in three different sections is provided: Whole organism (a and b), tail section (c and d) and intestine region (e and f). Asterisks indicate statistically significant differences to controls (*$p < 0.05$, **$p < 0.01$, and ***$p < 0.001$). Data are provided as mean and standard error of the mean (n=20).

However, embryos exposed to spherically shaped gold particles induced a reduced amount of neutrophils at the whole organism scale and in the tail region. Examination of the intestine (Figure 6.4e) learned that more neutrophils were present in embryos that were exposed to rods (compared to the control), whereas the embryos exposed to nanospheres again reduced the amount of neutrophils.

For the macrophages (Figure 6.4; b, d, f) at each examination level (whole body (b), tail (d) and intestine (f)) the embryos exposed to urchin shaped nanogold were observed to have a higher level of macrophages. For the embryos that were exposed to spherical nanogold particles, the overall abundance of macrophages was decreased for both the whole body and the tail region, whereas the intestine region had macrophages abundances that were comparable to the control.

The differently shaped particles showed different distribution patterns into the main digestive organs: gall bladder, pancreas and liver (Table 6.2). Embryos that had a high expression of either neutrophils or macrophages in the intestinal region, generally showed high abundance of immune cells in the gallbladder (Figure 6.5a), pancreas and / or liver (Figure 6; different combinations have been observed). The majority of the particles were transported to the pancreas, except for the nanospheres. Nanospheres were predominantly found within the liver. Nanospheres and nano-urchins were thereafter mostly found in the gall bladder, whereas nanorods and nano-bipyramids distributed mostly to the liver.

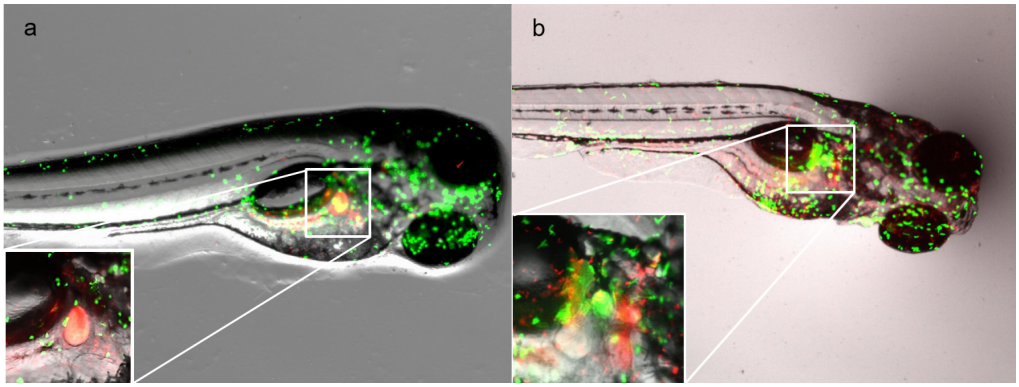

Figure 6.5: Images of fluorescent neutrophils (green) and macrophages (red) in zebrafish embryos after exposure to gold nano-bipyramids. The insets are providing further details using 2 times (*a*) and 6 times (*b*) magnification.

The observed distribution patterns (Table 6.2) were consistent with the observed abundance of immune cells (expressed as CTCF value) in the embryos (Figure 6.4): the nanorods and nano-urchins showed a high increase of the CTCF value in the intestine region and both shapes showed high abundancy of immune cells in the pancreas. In some cases, the immune cells accumulated more at the top of the pancreas, at the islets of Langerhans, rather

than accumulating in the whole pancreas (Figure 6.5b) For the nano-bipyramids, no obvious relation between the total amount of immune cells and the presence of immune cells in specific organs was observed. Exposure to nanospheres induced a reduction in the total amount of immune cells in the body as well as a strong reduction in fluorescent signal in the tail. However, no difference compared to the control was observed in fluorescent signal in the intestine region. This suggests that there was an overall reduction in the amount of immune cells and that the majority of the immune cells were translocated from the tail to the digestive organs and intestine.

	Gall bladder	Pancreas	Liver
Nanospheres	41 %	35 %	71 %
Nanorods	32 %	74 %	37 %
Nano-urchins	20 %	80 %	5 %
Nano-bipyramids	16 %	79 %	57 %

Table 6.2: Percentage of fish that showed high numbers of immune cells in the specified organs (n=19±1). Note that one single fish might be scored for multiple organs.

6.3.5 BEHAVIORAL RESPONSE

In order to investigate induced toxic effects related to the shape dependent biodistribution, a behavioral test was performed. The results of the behavior test showed that in the base phase a slight difference was observable with regard to the total distance that the hatched embryo moved (Figure 6.6). For embryos exposed to urchin shaped particles, the total distance moved was increased in the base phase whereas the other exposed groups did not show large differences, not even for the nano-bipyramids that also were predominantly found in the pancreas. In addition, accumulation of spherical particles in a high-energy demanding organ as the liver did not reduce the activity of the embryos. In the challenge phase, when stress was induced, embryos exposed to nano-bipyramids showed a reduced movement distance (Figure 6.6) and subsequent velocity (data not shown). On the other hand, the embryos exposed to nanorods traveled a longer distance per time interval and in total (Figure 6.6). In the recovery phase, the same tendency for the embryos exposed to nano-urchins as in the base phase was observed, although the effect is not so profound.

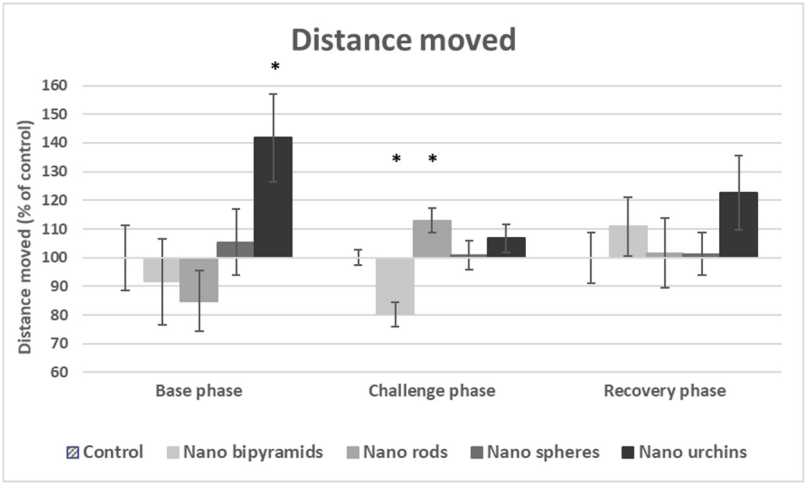

Figure 6.6: Total distance moved of 5dpf embryos exposed to different nanogold particles. Results are provided per stage of the behavior test (mean and standard error of the mean). Asterisks indicate significant differences to controls (*$p < 0.05$, **$p < 0.01$, and ***$p < 0.001$).

6.4 DISCUSSION AND CONCLUSION

The first question we aimed to answer is whether differently shaped Au-NPs are differently distributed within zebrafish embryos and whether the NPs reach different target organs. All shapes were found to accumulate on the intestinal mucosa. Yet adsorption to the intestinal mucosa is still not to be considered as either uptake or biodistribution. Evidence of the particles actually crossing the intestinal mucosa is provided by their presence in other digestive organs (such as the liver and gall bladder) as proven by confocal imaging. It should be noted that all differently shaped gold particles were found to be present in a blood vessel near the eye of the embryo. This is in line with our previous study[7], using fluorescent polystyrene (PS) particles with comparable size as the AuNPs tested in this study. Exposure to smaller (1.3 nm) AuNPs resulted in disruption of the growth and pigmentation of the eye of the embryos [34]. Due to high auto-fluorescence levels in the eye in our study, it was not feasible to examine the accumulation of gold in the eye. However, the presence and the mobility of the gold NPs in the blood veins, as shown by both our confocal imaging techniques, indicates a possibility of distribution throughout the organism and thus translocation to the eye.

Typically, xenobiotic particles that are taken up in the blood system are distributed throughout the organism and inflict harm to their host. To reduce or prevent harm, organisms evolved mechanisms to remove these particles from their body. For our second research question, we aimed to identify the clearance mechanism of the particles. As we saw in the time dynamic recording of the nano-bipyramids (Movie S1, SM), particles are taken up by macrophages and thereafter trafficking via the mononuclear phagocytic system (MPS). In general, spherical shaped particles show the fastest clearance rate compared to rod shaped particles [11], thereby favoring the hepatobiliary pathway over clearance via the kidneys [22,27]. Moreover, the clearance rate is further reduced when the particles are disk- or lamella-shaped [11], become more elongated [35], or develop sharp structures [13]. Once particles are taken up in macrophages, clearance via the MPS continues via the spleen, liver and eventually via bile trough the gallbladder into the digestive tract and feces [33]. In 5 dpf zebrafish embryos, the function of the spleen – which is not yet developed – is taken over by the pancreas [36]. Indeed, the pancreas, liver, gall bladder and digestive tract were found to contain nanoparticles. Just as for PSNPs [23], gold particles induced intestinal inflammation. Even more, induced activity of the innate immune system in the digestive organs was observed, which confirms the presence of the particles in these organs.

By using the immune response of the embryos, we aimed to answer our third research question: is the biodistribution reflected in different response patterns. Actually, a shape dependent pattern can be observed. Specifically focusing on the gall bladder, liver and pancreas, the distribution of the particles over these organs depends on particle shape. The differences across the distribution patterns indicate that the particles behave slightly different, although they

eventually reach the same target organs – yet in different ratios. In *in vitro* studies, the shape of the particle was shown to influence the rate of uptake and the circulation time, and subsequently the target organ [11]. Spherically shaped particles are most efficiently taken up compared to their rod and elliptical counterparts [11], whereas particles with sharp edges are capable of escaping the endosome and therewith prolonging their retention time [13]. Having a higher circulation time results in a larger probability to reach other target organs rather than the most prominent clearing organ – the liver [11]. As a matter of fact, the shape that was found to accumulate the most in the liver was the nanosphere.

The fourth question we aimed to answer is whether the biodistribution is reflected in the organismal behavior responses. The observed differences in the behavior test were only marginally significant and not always repeatable. As stated earlier by Browning et al. (2009), random internal distribution of individual gold nanoparticles into vital organs of the zebrafish can result in effects on the individual level while this is not a concentration dependent effect. After long-term exposure to PS NPs, particles were found to distribute into the brain where they modified brain tissue and subsequently changed behavior [37]. For that reason, exposure for a longer period might result in the presence of gold NPs in the brain of zebrafish, resulting in abnormal behavior patterns. Additionally, gold particles affecting the eye in early development induced behavioral effects [34]. With our exposure concentration, we were not able to observe any strong effects on the behavior, indicating that for this exposure period the concentration is too low to induce any behavioral effects. However, the nano-bipyramids reduced the total distance moved in the challenge phase, indicating that the embryos lack the energy to produce the full energy burst as seen in the control group. At the same time, no visible in- or decreases in immune levels were observed. This combination of observations suggests that the total energy budget of the organism is decreased, where the organisms allocates most of their energy to the immune response leaving less energy for locomotive responses. Reduction in locomotive responses is detrimental for the survival of an individual and it might even indicate a possible reduced fecundity due to a lack in energy. So, although we did not find strong effects of any of the gold nanoparticles on the behavior in zebrafish embryos after short exposure time, such effects might occur at higher concentrations, after long-term exposure or after exposure from the fertilization onwards.

Although some minor effects were observed, the different distribution patterns per particle shape did not induce significant sub-lethal effects. Since most studies report no cytotoxicity [38] nor toxicity [39] of gold particles, the absence of significant effects is not surprising. Often within drug delivery systems in which gold nanoparticles are used, surface modifications of the nanoparticles or protein labels are used to assist delivering the particle to the target organ. Over time, it might be likely that those surface modifications become unstable, and fractions of bare particles appear. The absence of sub-lethal effects due to bare and differently shaped gold nanoparticles strengthens the justification for utilizing gold nanomaterials as tracing agents in biodistribution studies and nanomedicine. We echo the suggestion made by Truong et al. (2015),

who stated on the basis of studying the biodistribution behavior more closely, that it will become possible to design particles that reach the desired target organ by choosing the appropriate particle shape. In this contribution, we showed that the biodistribution for all differently shaped gold NPs occurs rapidly via the circulatory system. However, harm remains limited, since the particles are distributed via the MPS towards the clearance organs where they are stored before elimination.

Internalized AuNPs were found to traffic throughout the blood system and reach via this medium most probably the whole organism. We observed presence of the particles in and trafficking via macrophages, indicating that the majority of the particles is removed via the MPS. Clearance via the MPS will result in biodistribution of particles in the digestive organs. In our study, exposure to differently shaped gold particles induced shape dependent biodistribution patterns. For each differently shaped particle, we found a different ratio in which they were distributed over the three assessed target organs: liver, gall bladder and pancreas. Although the particles were distributed differently over the examined digestive organs, in none of the cases major sub-lethal effects were observed. The biodistribution patterns indicated that long-term exposure might induce sub-lethal effects being shape-dependent. Finally, for nanosafety assessment, it is eminent that shape-features should be taken into account as a possible toxicity modifying factor as it affects the biodistribution patterns.

6.5 Supplementary Figures

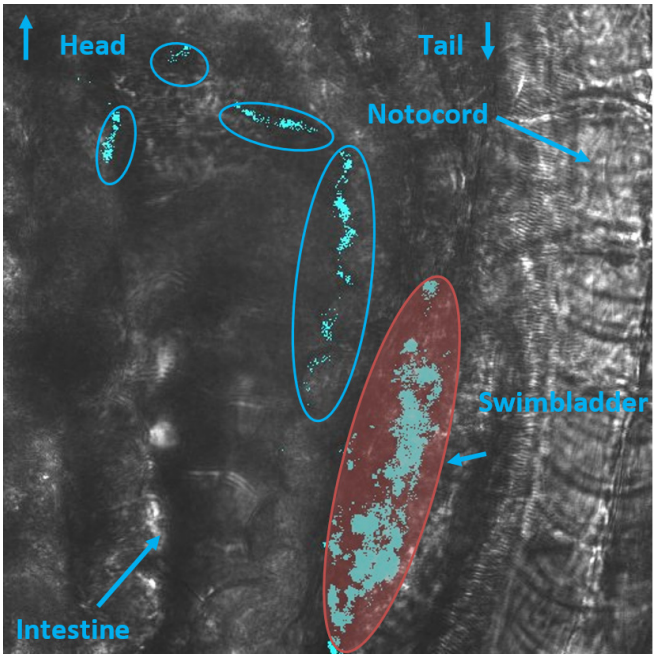

Figure S6.1: Confocal image of gold nano-urchin in different digestive organs. Autofluorescence in the swim bladder is marked red.

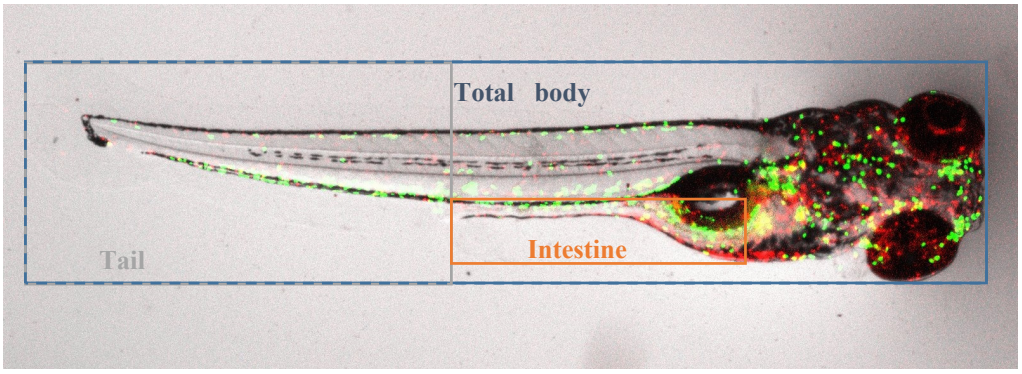

Figure S6.2 Image of a control fish with the different measurements areas used for the immune response assessment indicated: total body (blue), tail (green) and intestine (red).

6.6 BIBLIOGRAPHY

1. Handy, R. D., Henry, T. B., Scown, T. M., Johnston, B. D. & Tyler, C. R. Manufactured nanoparticles: their uptake and effects on fish--a mechanistic analysis. *Ecotoxicology* 17, 396–409 (2008).
2. Vijver, M. G. *et al.* Kinetics of Zn and Cd accumulation in the isopod Porcellio scaber exposed to contaminated soil and/or food. *Soil Biol. Biochem.* 38, 1554–1563 (2006).
3. Macrae, C. A. & Peterson, R. T. Zebrafish as tools for drug discovery. *Nat. Publ. Gr.* 14, 721–731 (2015).
4. Carnovale, C., Bryant, G., Shukla, R. & Bansal, V. Size, shape and surface chemistry of nano-gold dictate its cellular interactions, uptake and toxicity. *Prog. Mater. Sci.* 83, 152–190 (2016).
5. Gatoo, M. A. *et al.* Physicochemical properties of nanomaterials: implication in associated toxic manifestations. *Biomed Res. Int.* 2014, 498420 (2014).
6. Skjolding, L. M. *et al.* An assessment of the importance of exposure routes to the uptake and internal localisation of fluorescent nanoparticles in zebrafish (Danio rerio), using light sheet microscopy. *Nanotoxicology* 11, 351–359 (2017).
7. van Pomeren, M., Brun, N. R., Peijnenburg, W. J. G. M. & Vijver, M. G. Exploring uptake and biodistribution of polystyrene (nano) particles in zebrafish embryos at different developmental stages. *Aquat. Toxicol.* 190, 40–45 (2017).
8. Nazarenus, M. *et al.* In vitro interaction of colloidal nanoparticles with mammalian cells: What have we learned thus far? *Beilstein J. Nanotechnol.* 5, 1477–1490 (2014).
9. Black, K. C. L. *et al.* Radioactive 198Au-doped nanostructures with different shapes for in vivo analyses of their biodistribution, tumor uptake, and intratumoral distribution. *ACS Nano* 8, 4385–4394 (2014).
10. Huang, X. *et al.* The shape effect of mesoporous silica nanoparticles on biodistribution, clearance, and biocompatibility in vivo. in *ACS Nano* 5, 5390–5399 (2011).
11. Truong, N. P., Whittaker, M. R., Mak, C. W. & Davis, T. P. The importance of nanoparticle shape in cancer drug delivery. *Expert Opin. Drug Deliv.* 12, 1–14 (2015).
12. Qiu, Y. *et al.* Surface chemistry and aspect ratio mediated cellular uptake of Au nanorods. *Biomaterials* 31, 7606–7619 (2010).
13. Chu, Z. *et al.* Unambiguous observation of shape effects on cellular fate of nanoparticles. *Sci. Rep.* 4, 4495 (2014).
14. Khlebtsov, N. & Dykman, L. Biodistribution and toxicity of engineered gold nanoparticles: a review of in vitro and in vivo studies. *Chem. Soc. Rev.* 40, 1647–1671 (2011).

15. Takeuchi, I., Nobata, S., Oiri, N., Tomoda, K. & Makino, K. Biodistribution and excretion of colloidal gold nanoparticles after intravenous injection: Effects of particle size. *Biomed. Mater. Eng.* 28, 315–323 (2017).
16. Simpson, C. A., Huffman, B. J., Gerdon, A. E. & Cliffel, D. E. Unexpected toxicity of monolayer protected gold clusters eliminated by PEG-thiol place exchange reactions. *Chem. Res. Toxicol.* 23, 1608–1616 (2010).
17. Bogdanov, A. a *et al.* Gold Nanoparticles Stabilized with MPEG-Grafted Poly(l - lysine): in Vitro and in Vivo Evaluation of a Potential Theranostic Agent. *Bioconjug. Chem.* 26, 39–50 (2015).
18. Browning, L. M. *et al.* Random walk of single gold nanoparticles in zebrafish embryos leading to stochastic toxic effects on embryonic developments. *Nanoscale* 1, 138 (2009).
19. Arts, J. H. *et al.* A decision-making framework for the grouping and testing of nanomaterials (DF4nanoGrouping). *Regul. Toxicol. Pharm.* 71, S1–S27 (2015).
20. Mesquita, B. *et al.* Gold nanorods induce early embryonic developmental delay and lethality in zebrafish (Danio rerio). *J. Toxicol. Environ. Heal. - Part A Curr. Issues* 80, 672–687 (2017).
21. Bruinink, A., Wang, J. & Wick, P. Effect of particle agglomeration in nanotoxicology. *Arch. Toxicol.* 89, 659–675 (2015).
22. Kumar, R. *et al.* In vivo biodistribution and clearance studies using multimodal organically modified silica nanoparticles. *ACS Nano* 4, 699–708 (2010).
23. Brun, N. R. *et al.* Nanoparticles induce dermal and intestinal innate immune system responses in zebrafish embryos. *Environ. Sci. Nano* 5, 904–916 (2018).
24. Legradi, J., el Abdellaoui, N., van Pomeren, M. & Legler, J. Comparability of behavioural assays using zebrafish larvae to assess neurotoxicity. *Environ. Sci. Pollut. Res.* 22, 16277–16289 (2015).
25. OECD. *Validation report (phase 1) for the zebrafish embryo toxicity test, part I. Series on Testing and Assessment No. 157. ENV/JM/MONO(2011) 37. Paris, France* (2011).
26. van Pomeren, M., Peijnenburg, W., Brun, N. & Vijver, M. A novel experimental and modelling strategy for nanoparticle toxicity testing enabling the use of small quantities. *Int. J. Environ. Res. Public Health* 14, 1348 (2017).
27. Pan, Y. *et al.* High-sensitivity real-time analysis of nanoparticle toxicity in green fluorescent protein-expressing zebrafish. *Small* 9, 863–869 (2013).
28. Kim, C. S. *et al.* Cellular imaging of endosome entrapped small gold nanoparticles. *MethodsX* 2, 306–315 (2015).
29. Schindelin, J. *et al.* Fiji: an open-source platform for biological-image analysis. *Nat. Methods* 9, 676–82 (2012).
30. Balasubramanian, V., Srinivasan, R., Miskimins, R. & Sykes, A. G. A simple aza-crown ether containing an anthraquinone fluorophore for the selective detection of Mg(II) in living cells. *Tetrahedron* 72, 205–209 (2016).

31. van den Broek, B., Ashcroft, B., Oosterkamp, T. H. & van Noort, J. Parallel nanometric 3D tracking of intracellular gold nanorods using multifocal two-photon microscopy. *Nano Lett.* 13, 980–6 (2013)
32. Hua, J., Vijver, M. G., Ahmad, F., Richardson, M. K. & Peijnenburg, W. J. G. M. Toxicity of different-sized copper nano- and submicron particles and their shed copper ions to zebrafish embryos. *Environ. Toxicol. Chem.* 33, 1774–82 (2014).
33. Huwyler, J., Kettiger, H., Schipanski, A. & Wick, P. Engineered nanomaterial uptake and tissue distribution: from cell to organism. *Int. J. Nanomedicine* 8, 3255 (2013).
34. Kim, K. T., Zaikova, T., Hutchison, J. E. & Tanguay, R. L. Gold nanoparticles disrupt zebrafish eye development and pigmentation. *Toxicol. Sci.* 133, 275–288 (2013).
35. Sun, L. *et al.* Cytotoxicity and mitochondrial damage caused by silica nanoparticles. *Toxicol. Vitr.* 25, 1619–1629 (2011).
36. Danilova, N. & Steiner, L. A. B cells develop in the zebrafish pancreas. *Proc. Natl. Acad. Sci.* 99, 13711–13716 (2002).
37. Mattsson, K. *et al.* Altered behavior, physiology, and metabolism in fish exposed to polystyrene nanoparticles. *Environ. Sci. Technol.* 49, 553–561 (2015).
38. Chen, Y. *et al.* Gold nanoparticles coated with polysarcosine brushes to enhance their colloidal stability and circulation time in vivo. *J. Colloid Interface Sci.* 483, 201–210 (2016).
39. Asharani, P. V, Lianwu, Y., Gong, Z. & Valiyaveettil, S. Comparison of the toxicity of silver, gold and platinum nanoparticles in developing zebrafish embryos. *Nanotoxicology* 5, 43–54 (2011).